Elastic Scattering of 400-MeV Protons by ^{208}Pb

D. A. Hutcheon, J. M. Cameron, R. P. Liljestrand, P. Kitching, C. A. Miller, W. J. McDonald
D. M. Sheppard, W. C. Olsen, G. C. Neilson, and H. S. Sherif
Department of Physics, University of Alberta, Edmonton, Alberta T6G 2E1, Canada

and

D. K. McDaniels and J. R. Tinsley
Physics Department, University of Oregon, Eugene, Oregon 97403

and

L. W. Swenson
Physics Department, Oregon State University, Corvallis, Oregon 97331

and

P. Schwandt
Physics Department, Indiana University, Bloomington, Indiana 47405

and

C. E. Stronach
Physics Department, Virginia State University, Petersburg, Virginia 23803

and

L. Ray
Physics Department, University of Texas at Austin, Austin, Texas 78712
(Received 19 March 1981)

Cross-section and analyzing-power angular distributions for elastic scattering of 400-MeV protons by ^{208}Pb have been measured between 3° and 51°. Results have been compared to second-order Kerman-McManus-Thaler calculations of the optical potential. There is evidence that free nucleon-nucleon scattering amplitudes do not adequately describe nucleon propagation in nuclear matter at this energy.

PACS numbers: 25.40.Rb, 25.40.Cm

Elastic scattering of intermediate-energy protons is one of the better understood mechanisms which probe the distribution of matter in nuclei. At 0.8 and 1.0 GeV this process seems well described by multiple-scattering theory; the main uncertainty in neutron rms radii extracted at these energies stems from lack of detailed information about the nucleon-nucleon (N-N) interaction (especially the spin-dependent part), which is an input to the multiple-scattering calculations. At 400 MeV the N-N interaction is much better determined than at 800 and 1000 MeV and multiple-scattering calculations of total reaction cross sections[1] have indicated that the theory should still be applicable. Accordingly, we have collected proton + ^{208}Pb elastic scattering data at 400 MeV and compared them with multiple-scattering calculations, with the aim of testing the consistency of the model over an extended range of beam energies.

Differential cross sections and analyzing powers were measured with the 1.5-GeV/c magnetic spectrometer at the Tri-University Meson Facility. Scattering angles and solid angles were determined with use of a multiwire proportional chamber located at its entrance. In the angular range 2.8° to 20° the beam was stopped 1.2 m downstream of the target, and true zero in scattering angle could be found by a comparison of cross sections measured at positive and negative forward angles. For angles greater than 20°, the beam was stopped in an external dump and the true scattering angle was found by matching to small-angle data in a region of overlap. We estimate the angles to be accurate to $\pm 0.1°$ and the angular resolution to be $\pm 0.2°$. The energy resolution of 1.0 MeV full width at half maximum was sufficient to eliminate inelastic proton scattering and a time-of-flight cut removed any background due to deuterons or tritons having the same momentum as the elastically scattered protons.

Beam intensity and polarization were monitored by an in-beam polarimeter, and several checks of normalization were made by measuring proton-proton elastic scattering from a CH_2 target. The beam polarization was typically 0.65 to 0.70 with an estimated uncertainty of ± 0.015, and the cross sections were determined with relative errors of $\pm 4\%$ and a systematic uncertainty of $\pm 7\%$.

Angular distributions of cross section and analyzing power, measured from 2.8° to 52° (lab), are shown as points in Fig. 1. As in other intermediate-energy measurements the cross sections show oscillations characteristic of diffraction. The analyzing-power angular distribution has deep minima, reaching negative values similar to observations at 161 and 181 MeV,[2] and unlike the 800-MeV distribution,[3] which is always positive.

The curves of Fig. 1 are Kerman-McManus-Thaler (KMT) optical-potential calculations[4] which were performed assuming local, spin-dependent forms for both first- and second-order terms. The 400-MeV proton-proton amplitudes of Arndt[5] and the 400-MeV proton-neutron amplitudes of Bystricky, Lechanoine, and Lehar[6] have been used. The proton density was determined from the model-independent ^{208}Pb charge density of Frois *et al.*[7,8] Several corrections to the impulse approximation have been included: (1) Pauli blocking,[9] (2) Fermi motion averaging, assuming a Fermi-gas density matrix,[10] (3) nonlocality due to the dependence on incident momentum of the optical potential,[11] and (4) Pauli, short-range dynamical, and center-of-mass correlations between the target nucleons.[8] The Coulomb interaction was handled according to Ray, Hoffman, and Thaler.[12]

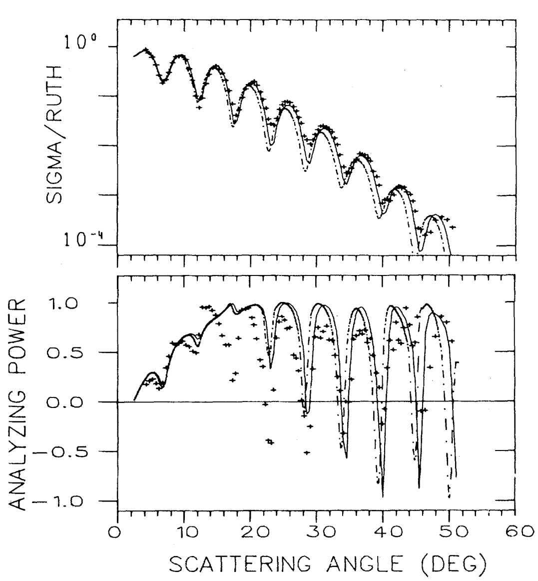

FIG. 1. Cross-section and analyzing-power angular distributions measured in this experiment. The curves are second-order KMT optical-model calculations based on the neutron density distribution of Eq. (1) (broken line), or a three-parameter Gaussian distribution (solid line). The cross sections have been divided by the Rutherford scattering cross section.

The dashed curves of Fig. 1 are KMT calculations based on a neutron density

$$\rho_n^{\mathrm{theory}}(r) = \rho_n^{\mathrm{DME}}(r) + \rho_p^{\mathrm{Exp}}(r) - \rho_p^{\mathrm{DME}}(r), \qquad (1)$$

where DME refers to the density matrix expansion of Negle and Vautherin[10] and ρ_p^{Exp} is the empirical proton density. That is, the theoretical neutron density is assumed to differ from that predicted by DME in the same way that the empirical proton density differs from the DME proton density. This theoretical prediction provides a good description of the angular distribution data inside 12° c.m., but becomes out of phase and exhibits cross-section minima which are too deep when compared with the larger-angle data. By adjusting a three-parameter Gaussian model of neutron density,[3] we obtain an improved fit to the cross sections as shown by the solid line of Fig. 1. The cross sections and analyzing powers predicted by the two neutron densities are very similar, except for the angular period of oscillations. For comparison, the root-mean-square radii are as follows: theoretical neutron density, 5.65 fm; the three-parameter Gaussian fitted neutron distribution, 5.42 ± 0.10 fm; the neutron density obtained from a similar three-parameter Gaussian analysis of 800-MeV proton scattering data[3] with use of the phase shifts of Arndt,[5] 5.50 ± 0.05 fm; and the ^{208}Pb proton density, 5.45 fm. The contributions to uncertainty in our result are given in Table I.

Neither neutron distribution predicts the deep minima in analyzing power in the middle part of the angular distribution, in much worse disagreement than at 800 MeV.[13] This raises concern about the applicability of the KMT model to our data and, in turn, the reliability of the deduced neutron distributions. One might question the use of the KMT model at 400 MeV, or whether free nucleon-nucleon amplitudes adequately describe proton propagation in nuclear matter, for example. We have done a demonstration calculation to examine one aspect of the latter point, namely the Pauli blocking correction. In the KMT calculation the Pauli blocking correction was estimated with use of a noninteracting Fermi-gas

TABLE I. Contributions to uncertainty in neutron rms radius.

Source	Magnitude	Contributions to rms radius error (fm)
Normalization	± 7.5%	± 0.015
Scattering angle	± 0.1°	± 0.056
Beam energy	± 1 MeV	± 0.013
Proton rms radius	± 0.01 fm	± 0.005
Statistical uncertainty		± 0.03
Nucleon-nucleon amplitudes		± 0.033
Correlation correction		± 0.02
Total		± 0.10

model, and resulted in a small, density-dependent reduction in the strength of the central potential. We have investigated the effect of arbitrarily increasing the strength of this correction, adding it to the first-order KMT term. Calculated analyzing powers are changed significantly, being in better agreement with data at middle angles but shifted too low at back angles, as shown in Fig. 2. This modification does not shift positions of maxima in either cross section or analyzing power, and its effect on cross sections is to deepen the minima, resulting in poorer agreement with large-angle data. The effect of the "correction" on the real part of the optical potential, plotted in Fig. 3, is to change it from attractive to repulsive in the medium- and high-density parts of the nucleus; the volume integral changes from $J_R/A = -70$ to $+10$ MeV fm^3. On the other hand, the "correction" produces relatively little change in the shape of the imaginary part of the optical potential.

We do not suggest that this calculation should be used in determining neutron rms radii—there is no theoretical justification for the precise form and strength of this Pauli term, and agreement with large-angle data is made worse. Its value lies rather in its demonstration of the type of potential which will improve the middle-angle analyzing-power predictions, the most conspicuous shortcoming of the second-order KMT calculations. In radial dependence of the central potential it is similar to results in lighter nuclei obtained in Brueckner-Hartree-Fock and Dirac-Hartree calculations.[14] In these models the real central potential is less attractive (or even repulsive) in the nuclear interior than at the surface

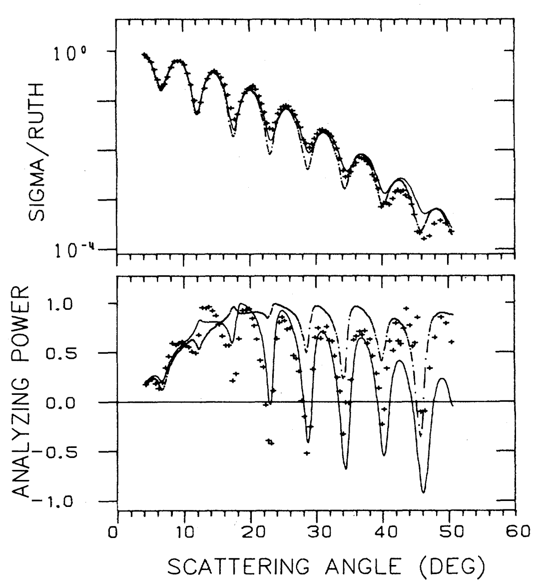

FIG. 2. Comparison of our data with a KMT calculation having a Pauli blocking correction of enhanced strength (solid line), or having first-order terms only (broken line). The cross sections have been divided by the Rutherford scattering cross section.

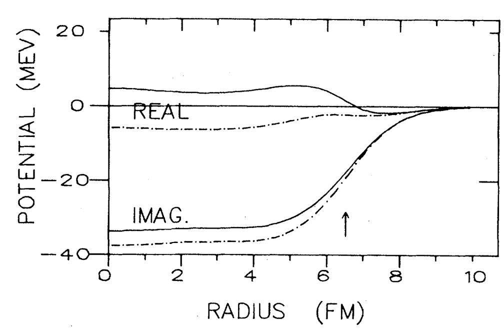

FIG. 3. Radial dependence of the central potentials generated by the KMT calculations shown in Fig. 2, containing enhanced Pauli blocking correction (solid lines) or first-order terms only (broken lines). The arrow indicates the radius at which the nuclear density is one-half the central value.

for proton energies of 150 to 500 MeV.

In summary, we draw the following conclusions from our 400-MeV $p+{}^{208}$Pb results: (1) A KMT optical potential for which the real central part has a radial form closely resembling that of the matter density, as is derived with use of free N-N amplitudes, does not give correct analyzing powers. (2) Improved prediction of analyzing powers seems to require that the potential does not simply vary linearly with matter density. Such potentials arise naturally in Brueckner-Hartree-Fock or Dirac-Hartree models, and such models may be necessary to explain elastic scattering of protons at 400 MeV. (3) The positions of maxima and minima in the cross-section angular distribution depend sensitively on the rms radius of the neutron density, but not on a density-dependent modification to the effective N-N interaction. Whatever the deficiencies in the KMT model turn out to be at 400 MeV, it is possible that they do not affect neutron radius determinations; our result for the rms neutron radius of ^{208}Pb is within a standard deviation of that obtained at 800 MeV, and significantly lower than the prediction of the density matrix expansion model.

The interest and encouragement of Dr. J. S. Blair during the early state of this experiment is gratefully acknowledged. This work was supported in part by the Natural Sciences and Engineering Research Council of Canada, the U. S. National Aeronautics and Space Administration, and the U. S. Department of Energy.

[1]L. Ray, Phys. Rev. C 20, 1857 (1979).
[2]A. Nadasen *et al.*, Indiana University Cyclotron Facility Report No. 118 (to be published), and Phys. Rev. C 23, 2353 (1981).
[3]G. W. Hoffmann *et al.*, Phys. Rev. C 21, 1488 (1980).
[4]A. K. Kerman, H. McManus, and R. M. Thaler, Ann. Phys. (N.Y.) 8, 551 (1959).
[5]R. A. Arndt, private communication. (We used solution SM80 of 15 July 1980).
[6]J. Bystricky, C. Lechanoine, and F. Lehar, Saclay Report No. D-Ph-PE-79-01, 1979 (unpublished).
[7]B. Frois *et al.*, Phys. Rev. Lett. 38, 152 (1977).
[8]L. Ray, Phys. Rev. C 19, 1855 (1979).
[9]E. Clementel and C. Villi, Nuovo Cimento 2, 176 (1955).
[10]J. W. Negele and D. Vautherin, Phys. Rev. C 5, 1472 (1972).
[11]B. Mulligan, Ann. Phys. (N.Y.) 26, 159 (1964).
[12]L. Ray, G. W. Hoffmann, and R. M. Thaler, Phys. Rev. C 22, 1454 (1980).
[13]G. W. Hoffmann *et al.*, Phys. Lett. 40, 1256 (1978).
[14]M. Jaminon, C. Mahaux, and P. Rochus, Phys. Rev. C 22, 2027 (1980); C. Mahaux, in *Common Problems in Low and Medium Energy Nuclear Physics*, edited by B. Castel, B. Goulard, and F. C. Khanna (Plenum, New York, 1979), p. 265.

Investigation of the Fission Decay of the Isoscalar Giant Quadrupole Resonance in ^{238}U by Electron- and Positron-Induced Fission

H. Ströher, R. D. Fischer, J. Drexler, K. Huber, U. Kneissl, R. Ratzek, H. Ries, and W. Wilke
Institut für Kernphysik, Strahlenzentrum der Universität Giessen, D-6300 Giessen, West Germany

and

H. J. Maier
Universität München, D-8000 München, West Germany
(Received 4 June 1981)

The controversial results for the fission decay of the isoscalar giant quadrupole resonance in ^{238}U have been investigated by electron- and positron-induced fission experiments ($E_e = 10-35$ MeV). The measured cross-section ratio σ^-/σ^+ and absolute cross sections were analyzed with use of available distorted-wave Born-approzimation virtual-photon spectra. Within this analysis no fission decay of the giant quadropole resonance could be detected, in contrast to a recent inclusive electrofission work.

PACS numbers: 25.85.Jg, 24.30.Cz, 27.90.+b

The isoscalar giant quadrupole resonance (GQR) in heavy nuclei[1] has been observed in various hadron- and electron-induced reactions[2-4] at an excitation energy of $\approx 65A^{-1/3}$ MeV. However, a number of controversial experiments have been recently reported on the fission decay of the GQR